

## Article

# Mechanical and Tribological Performance of Epoxy Composites Reinforced with YSZ Waste Ceramics for Sustainable Green Engineering Applications

Talal Alsaeed <sup>1</sup>, Ayedh Eid Alajmi <sup>2</sup>, Jasem Ghanem Alotaibi <sup>2</sup> , Voravich Ganthavee <sup>3</sup>  and Belal F. Yousif <sup>3,\*</sup> 

<sup>1</sup> Department of Manufacturing Engineering Technology, Public Authority for Applied Education and Training, Kuwait City 70654, Kuwait; ts.alsaeed@paaet.edu.kw

<sup>2</sup> Department of Automotive and Marine Engineering Technology, Public Authority for Applied Education and Training, Adailiyah 42325, Kuwait; ae.alajmi@paaet.edu.kw (A.E.A.); jg.alotaibi@paaet.edu.kw (J.G.A.)

<sup>3</sup> School of Engineering, University of Southern Queensland, Toowoomba, QLD 4350, Australia; voravich.ganthavee@unisuq.edu.au

\* Correspondence: belal.yousif@usq.edu.au; Tel.: +61-7463-15331

**Abstract:** The growing need for sustainable materials in engineering applications has led to increased interest in the use of waste-derived ceramics as reinforcing fillers in polymer composites. This study investigates the mechanical and tribological performance of epoxy composites reinforced with Yttria-Stabilized Zirconia (YSZ) waste ceramics, focusing on the effects of varying ceramic content (0–40 wt.%). The results demonstrate that while the tensile strength decreases with increasing ceramic content, the wear resistance and surface hardness improve, particularly at 20 wt.% YSZ. These findings are highly relevant for industries such as automotive, aerospace, and industrial manufacturing, where the demand for eco-friendly, high-performance materials is growing. This work aligns with the journal's focus on sustainable engineering by offering new insights into the practical application of waste materials in high-performance composite systems.

**Keywords:** tensile; wear; epoxy; friction; ceramic



**Citation:** Alsaeed, T.; Alajmi, A.E.; Alotaibi, J.G.; Ganthavee, V.; Yousif, B.F. Mechanical and Tribological Performance of Epoxy Composites Reinforced with YSZ Waste Ceramics for Sustainable Green Engineering Applications. *Processes* **2024**, *12*, 2609. <https://doi.org/10.3390/pr12112609>

Academic Editors: Maria José Lo Faro and Mostafa Y. Nassar

Received: 10 September 2024

Revised: 13 November 2024

Accepted: 18 November 2024

Published: 20 November 2024



**Copyright:** © 2024 by the authors. Licensee MDPI, Basel, Switzerland. This article is an open access article distributed under the terms and conditions of the Creative Commons Attribution (CC BY) license (<https://creativecommons.org/licenses/by/4.0/>).

## 1. Introduction

The need for materials that adhere to environmental rules is required, especially in industrialized nations. Pollution brought on by the manufacture of materials and the disposal of trash is a concern of governments and academics. In addition, the extraction, manufacture, application, and disposal of materials all demand a considerable amount of energy [1–4]. There has been an increase in novel material research and development that complies with environmental control criteria. The manufacture of materials could be revolutionized by these new materials, making it more environmentally responsible and sustainable. Scientists are exploring the potential of various materials that are less energy-intensive and produce less waste for a more sustainable future [5–8].

The potential of waste ceramics in engineering applications has been investigated in several studies, either as aggregates [9–11] or in powder form [12–14]. Recent research has also explored the potential of ceramics in polymer composites [15–17]. The advantages of utilizing waste ceramics in polymer composites included improvements in the characteristics of ceramic and polymer materials when mixed. In Robinson et al. [18], there were positive interactions between the created materials and the human body, and notable improvements in mechanical properties. These results highlight the significance of additional research and development in this field and point to the potential of waste ceramics in a variety of fields.

Design and engineering applications rely heavily on tribology, especially in mechanical systems fields [19,20]. Designing key components with low wear rates and great reliability,

such as bearings, gears, and valves, requires good tribological performance of materials. In other words, tribology is a crucial field of study that permits the development of effective, dependable, and environmentally friendly technology [21,22].

On the other hand, epoxy composites have drawn much interest because of their superior mechanical and thermal characteristics, making them appropriate for a wide range of industrial applications. Epoxy composites' wear behavior, though, is a major worry for their dependability and longevity. When two surfaces come into contact and move relative to one another, wear occurs, leading to material loss or deformation [23]. In epoxy composites, variables like the kind and quantity of reinforcing fillers, the sliding distance, and the load conditions affect the wear mechanisms. Researchers have investigated several techniques to increase the wear resistance of epoxy composites [24], including adding nanofillers [25], changing the fillers' surface chemistry, and optimizing the manufacturing conditions [26]. These methods have shown notable improvements in the wear behavior of epoxy composites, offering new applications where high wear resistance is essential to present prospects for their utilization. Therefore, for epoxy composites to be successfully used in engineering applications, understanding their wear behavior is crucial.

Many studies have investigated the use of ceramic fillers in polymer composites due to their ability to enhance mechanical and thermal properties. Yttria-Stabilized Zirconia (YSZ), in particular, has been widely studied for its high wear resistance and hardness [27–29]. However, most of these studies focus on the use of commercial YSZ and do not explore the potential of waste-derived YSZ as a sustainable material for reinforcing epoxy composites. Moreover, while the mechanical properties of ceramic-filled composites have been extensively studied, there is limited research on their tribological behavior—specifically, how ceramic content influences friction and wear performance in high-wear environments such as industrial applications [30,31].

The primary objectives of this study are threefold. First, we aim to explore the potential of waste-derived Yttria-Stabilized Zirconia (YSZ) as a reinforcing filler in epoxy composites, focusing on its role in enhancing the material's mechanical and tribological properties. Second, we seek to evaluate how varying YSZ content (0–40 wt.%) affects the composite's overall performance, particularly in terms of strength, the modulus, wear resistance, and the friction coefficient. Third, this study assesses the feasibility of utilizing YSZ-reinforced epoxy composites in sustainable engineering applications, with an emphasis on their potential contributions to industries that require high-performance, eco-friendly materials. These objectives guide the research and ensure a focus on both the scientific and practical implications of incorporating waste ceramics into composite materials.

This study presents an innovative approach by combining waste-derived Yttria-Stabilized Zirconia (YSZ) ceramics, tribological analysis, and epoxy composites to offer a sustainable engineering solution. The integration of YSZ waste in epoxy composites not only addresses environmental concerns by reducing industrial waste but also enhances the tribological properties of the composite, making it suitable for applications where wear resistance is critical. This novel combination of waste materials with tribological engineering presents a significant advancement in the development of eco-friendly materials that can contribute to sustainable manufacturing practices. The novelty of this study lies in the use of waste-derived Yttria-Stabilized Zirconia (YSZ) as a sustainable reinforcing material in epoxy composites. Unlike previous research that primarily utilizes commercial ceramic fillers, this study focuses on repurposing industrial ceramic waste to address both environmental concerns and material performance. Furthermore, this research not only examines the mechanical properties of YSZ/epoxy composites but also provides a comprehensive evaluation of their tribological performance under varying ceramic content. By identifying the optimal YSZ content (0–40 wt.%) for achieving a balance between wear resistance and mechanical properties, this study contributes new insights into the design of eco-friendly, high-performance composites for industrial applications.

## 2. Material Preparation and Experimental Details

### 2.1. Material Selection

For the waste ceramic selection, Yttria-Stabilized Zirconia zirconium oxide ceramic nanopowder was selected for the current study. Zirconium oxide, a kind of nanoscale Yttria-Stabilized Zirconia, is typically 5 to 100 nm in size and has a specific surface area (SSA) of 25 to 50 m<sup>2</sup>/g. High-performance epoxy was used; the commercial name is platinum marine epoxy (5:1 mixing ratio). Platinum marine epoxy is a practical and convenient option for repair and building projects as recommended by the Aero marine product. The primary materials used in this study were Yttria-Stabilized Zirconia (YSZ) powder and epoxy resin. The YSZ powder (chemical formula: ZrO<sub>2</sub> stabilized with 8 mol% Y<sub>2</sub>O<sub>3</sub>) was obtained as a waste byproduct from Zhengzhou Xinli Wear-Resistant Material Co., Ltd. (Zhengzhou, China), which specializes in the production of ceramic coatings and wear-resistant materials for industrial applications. The waste YSZ was no longer viable for its original use due to performance degradation during the manufacturing process. While the powder retained its general YSZ structure, it may have contained minor impurities such as residual binder materials or trace elements from the production process. These potential impurities were not expected to significantly impact the composite's performance for the scope of this study.

### 2.2. Composite Fabrication

The current fabrication process of YSZ ceramic/epoxy composites utilizes a molding technique. The steps are displayed in Figure 1. Two separate molds are employed to fabricate tensile and tribological samples, respectively. The requisite equipment and materials for this process are delineated in Figure 1a,b. Initially, the mixture of epoxy resin and hardener is prepared, a measured amount of YSZ ceramic is added (0 wt.–40 wt.%), and then the mixture is homogenized using electrical mixing to ensure an even distribution of the filler material within the composites. A weight scale was used to calculate the required amount of all the YSZ ceramics at an accuracy of ±0.01 mg. The content percentage of the ceramic in the epoxy was determined by weight. The prepared epoxy mixture was weighted, and the required amount of ceramic was added to the mixture accordingly.

The preparation of the epoxy composites involved a standard molding process per ASTM D638 and ASTM G99 standards [32,33] for tensile and tribological testing, respectively [34–36]. The epoxy resin and hardener were mixed at a 5:1 ratio, and YSZ ceramic powder was added in varying amounts (0 wt.% to 40 wt.%). The mixture was poured into molds and cured at ambient temperature for 24 h, followed by post-curing at 100 °C.

The selection of ceramic content was guided by previous studies [37–39] indicating that higher ceramic loadings (up to 40 wt.%) can significantly influence mechanical properties, particularly in terms of wear resistance and surface hardness. The range of YSZ content (0–40 wt.%) was chosen to explore how different levels of ceramic reinforcement affect both the mechanical and tribological behavior of the composites. The testing parameters, such as a sliding speed of 3 m/s and an applied load of 30 N for tribological tests, were selected based on the operational limits of epoxy composites in industrial applications where wear and friction are critical concerns.

### 2.3. Experimental Setup and Procedure

The widely used standard test technique ASTM D638 was used to evaluate the tensile characteristics of the epoxy composites [32]. Calculations of the modulus of elasticity, ultimate tensile strength, and ductility were carried out using the obtained data from the machine. A loading rate of 2 mm/min was set up in the machine, and for each set of samples there are four repeated tests, and the average value of the properties are calculated. Table 1 presents the experimental parameters for both tensile and tribological tests.

For the tribological experiments, different epoxy composites containing 0–40% ceramic in the testing of the samples were evaluated. The tribological machine was set up in the configuration of the block on the ring to experiment with different sliding distances with

applied loads of 30 N and a sliding speed of 3 m/s, which is within the limit of the Pressure  $\times$  Velocity (PV) of the epoxy. The sliding distance varied from 2 km up to 11 km to determine the steady state of the specific wear rate of the samples. To achieve the required surface roughness of below 1  $\mu\text{m}$  for adhesive wear condition, the prepared samples were smoothed with sandpaper of 1500 grade. The counterface was made of stainless steel, which was polished with the same grade of sandpaper to ensure the interaction of the asperities in adhesive condition. Before and after each test, the samples were weighed using a high-precision weight scale of 0.001 mg accuracy to determine the weight loss and then the specific wear rate. The friction coefficient was determined based on the applied load and the measured frictional force using a load cell via a data acquisition system.

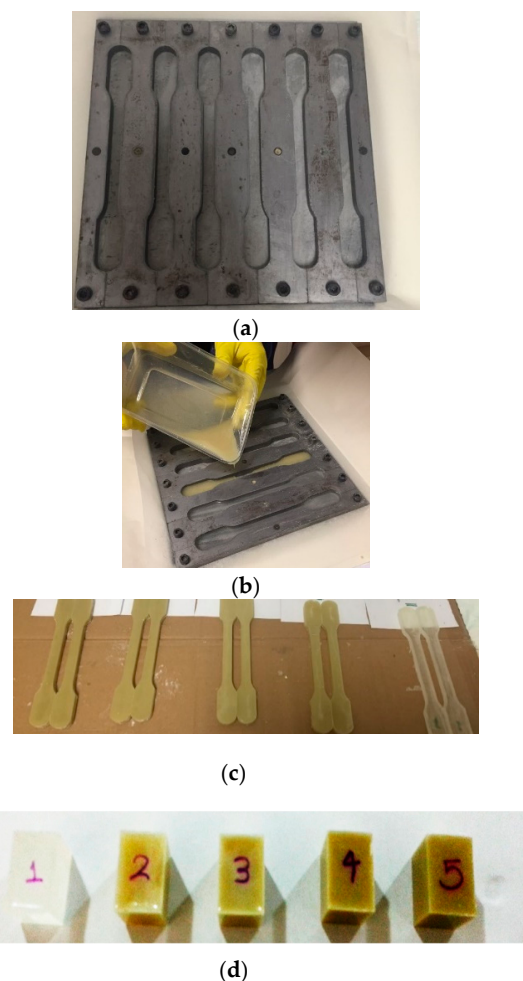


**Figure 1.** Sample preparation and experimental specimens. (a) Photo of the tensile mold; (b) photo of pouring the composite mixture into the tensile mold; (c) photo of the tensile specimens; and (d) photo of the tribological specimens.

The specific wear rate (SWR) is determined using the following formula:

$$\text{SWR} = \Delta V / (F \cdot D)$$

where

$\Delta V$ : change in volume of the material ( $\text{mm}^3$ );

F: applied force (N);

and D: sliding distance (m).

The damages on the surfaces of the samples after the tests were observed using scanning electron microscopy (Joel). Before the SEM observation, the samples were coated

with gold using a Smart Counter Machine. The surface roughness of the counterface and the worn surface were measured to determine the modifications that took place on the surfaces after the tribological loadings.

**Table 1.** Summary of the experimental work.

Experiment	Parameter	Value/Setting
Tensile Test	Standard Test Technique	ASTM D638
	Loading Rate	2 mm/min
	Number of Repeated Tests	4
Tribological Experiment	Composite Composition	Epoxy composites containing 0–40% ceramic
	Testing Configuration	Block on Ring
	Applied Load	30 N
	Sliding Speed	3 m/s
	Sliding Distance Range	2 km to 11 km
	Surface Roughness, Ra	Below 1 $\mu\text{m}$
	Counterface Material	Stainless steel

### 3. Results and Discussion

Figure 2 and Table 2 describe the spectral differences between the pure sample and 20% and 40% ceramic/epoxy composites. The results show that the strong vibration characteristic peak at  $3500\text{ cm}^{-1}$  can be attributed to the tensile vibration of -OH on the YSZ waste ceramic or zirconia surface. The strong, sharp vibration peaks, such as at  $3741.90\text{ cm}^{-1}$  and  $3834.49\text{ cm}^{-1}$ , are silanol groups. The characteristic absorption peaks at  $2360.87\text{ cm}^{-1}$ ,  $1697.36\text{ cm}^{-1}$ ,  $1519.91\text{ cm}^{-1}$ , and  $749\text{ cm}^{-1}$  indicate the presence of -OH tensile vibration in  $\text{SiO}_2\text{H}$ , C=O stretching in the amino ester -O-C(O)-NH-, and -C=C- and Zr-O-Zr tensile vibration, respectively. As the zirconia ceramic content or filler content increases, the degree of cross-linking also increases. In conclusion, the presence of these surface chemical functional groups indicates that the epoxy resin successfully anchored on the surface of YSZ waste ceramics or zirconia, supported through chemical bonding.

**Table 2.** Characteristic absorption peaks of ceramic/epoxy composites.

IR (Frequency, $\text{cm}^{-1}$ )	Ceramic/Epoxy Composites
Geminal -OH vibration	$3741.90\text{ cm}^{-1}$ , $3834.49\text{ cm}^{-1}$
Free -OH vibration	$3675\text{--}3670\text{ cm}^{-1}$
Out-of-phase OH tensile vibration of adjacent SiOH groups in inter-molecular cyclic configuration	$3650\text{ cm}^{-1}$
In-phase OH tensile vibration of adjacent SiOH groups in inter-molecular cyclic configuration	$3620\text{ cm}^{-1}$
-OH vibration on $\text{ZrCO}_2$ surface	$3403\text{ cm}^{-1}$
-OH tensile vibration in $\text{SiO}_2\text{H}$ intra-molecular cyclic configuration	$2360.87\text{ cm}^{-1}$
C=O stretching; -O-C(O)-NH-	$1697.36\text{ cm}^{-1}$
-C=C- stretching	$1519.91\text{ cm}^{-1}$
-CH <sub>2</sub> -, -CH <sub>3</sub> - asymmetric stretching	$2927\text{ cm}^{-1}$ , $2968\text{ cm}^{-1}$
-CH <sub>2</sub> -, -CH <sub>3</sub> - symmetric stretching	$2856\text{ cm}^{-1}$ , $2873\text{ cm}^{-1}$
Si-O-Si, siloxane	$1115\text{ cm}^{-1}$
Zr-O-Si	$958\text{ cm}^{-1}$
Zr-O-Zr	$749\text{ cm}^{-1}$

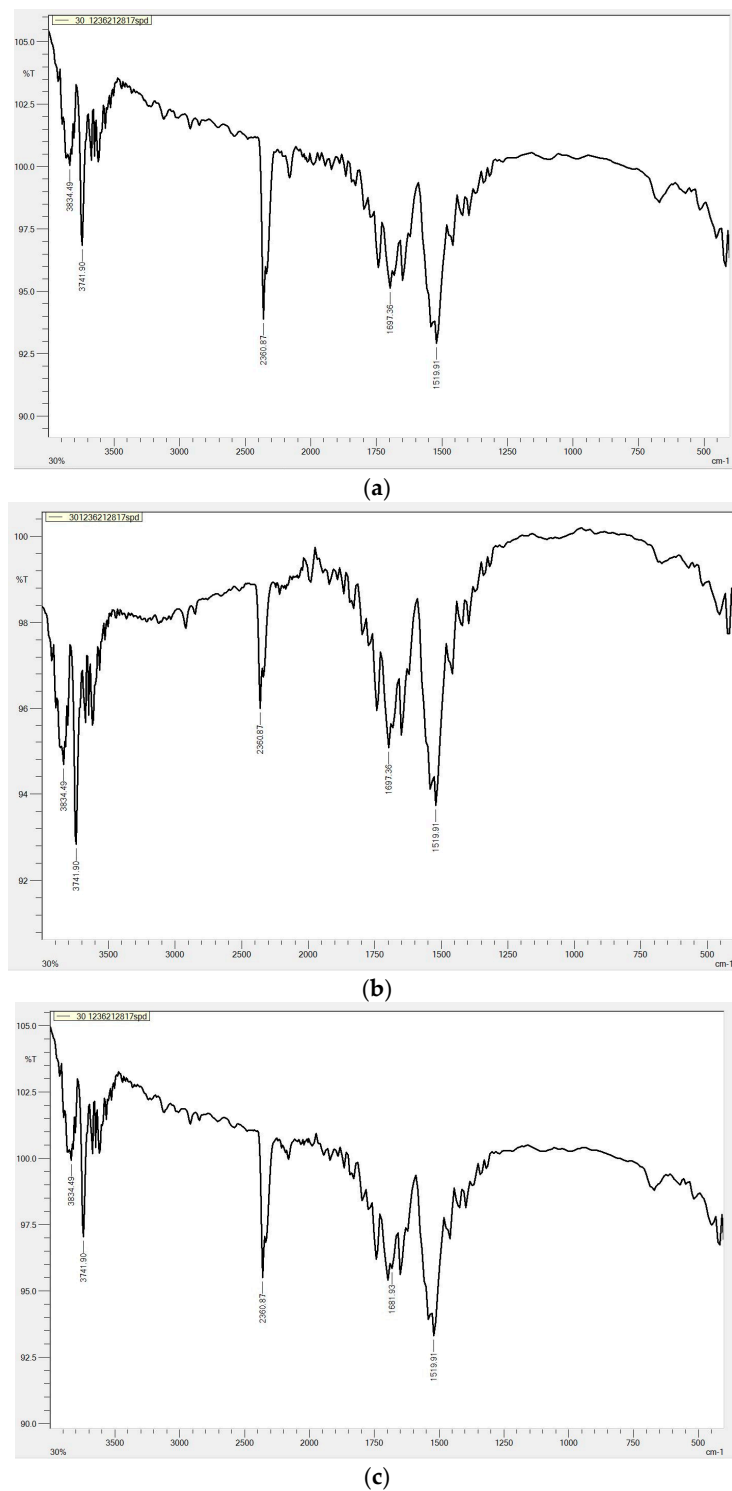


**Figure 2.** Fourier Transform Infrared (FTIR) spectroscopy of (a) pure epoxy, (b) 20% ceramic ceramic/epoxy composites, and (c) 40% ceramic/epoxy composites.

### 3.1. Tensile Results

The stress–strain curves shown in Figure 3 illustrate the tensile behavior of epoxy composites with different YSZ ceramic contents. The blue lines correspond to composites with lower ceramic content (e.g., 0–20 wt.%), which exhibit a more ductile behavior, characterized by a greater strain before failure. In contrast, the orange lines represent composites with higher ceramic content (30–40 wt.%), where the material exhibits a more brittle response, failing at lower strains. This transition is due to the increased ceramic content,

which reduces the matrix's ability to deform plastically and results in more brittle fracture behavior [40,41]. The clear separation of the curves allows for a detailed comparison of how ceramic content influences mechanical performance.

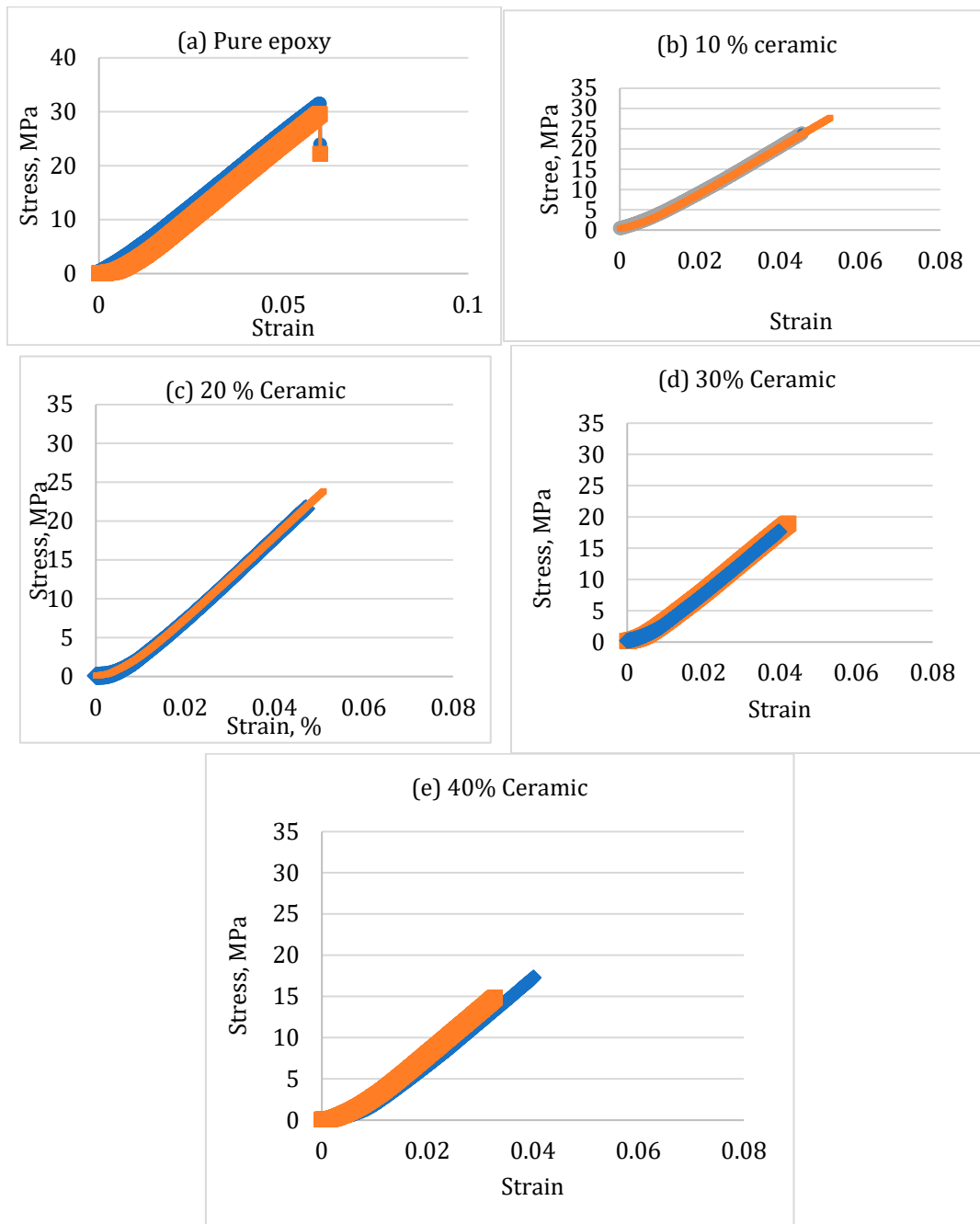


**Figure 3.** Stress (MPa) vs. strain for composite containing different weight percents of YSZ ceramic.

The raw data (force vs. deformation) were converted to a stress–strain diagram and are presented in Figure 3a–e for epoxy/ceramic composites with varying ceramic contents (0 wt.%–40 wt.%). Each figure corresponds to a set of experiments for the same content of ceramic in the composite. The data were collected by subjecting the samples to a tensile load until fracture occurred. It should be mentioned here that at the initial stage of the loading, a gripping process took place. This gripping process is a natural behavior that occurs during the initial stage of tensile testing [42]. The general behavior of all composites showed a brittle nature since plastic deformation is absent, i.e., the composites were not

able to undergo significant deformation without cracking or breaking. Furthermore, the variations in the trends and values of each set of experiments were minimal for each set of tests. This indicates that the fabrication of the composites was performed with a high degree of precision, resulting in minor errors. The ultimate tensile strength, ductility, and modulus of elasticity of the epoxy composites are presented in Figure 4a–c.

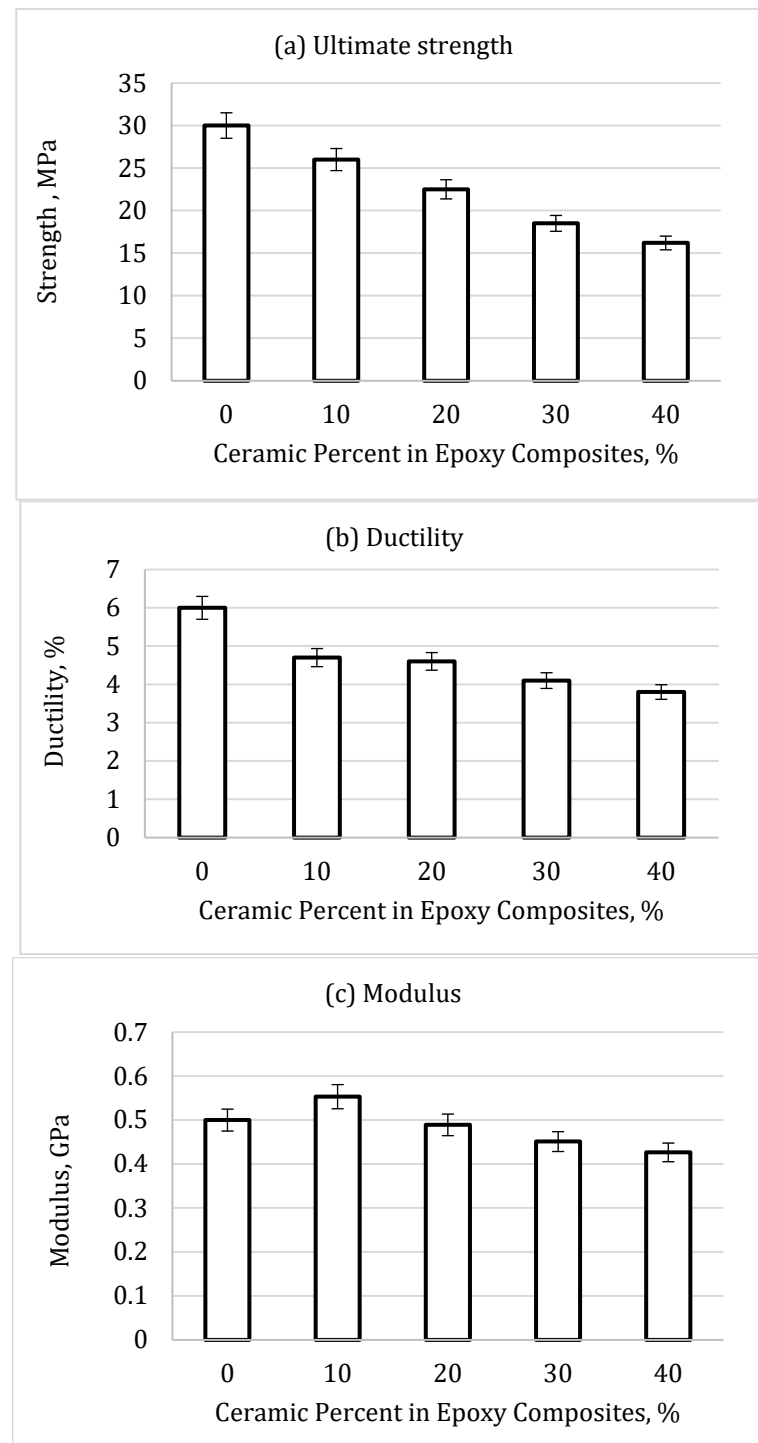


**Figure 4.** Ultimate strength, ductility, modulus of elasticity for epoxy composites containing different percentages of ceramic.

The ultimate tensile strength of epoxy/ceramic composites is in the range of 18 MPa to 30 MPa. Pure epoxy shows an average tensile strength of 30 MPa. The addition of 10 wt.%

of ceramic powder reduces the strength to about 27 MPa. Furthermore, the increase in the ceramic content deteriorates the tensile strength of the epoxy composites. Pure ceramic has a tensile strength above 100 MPa; therefore, the deterioration of the strength with the addition of the ceramic in the epoxy composites may be due to the adhesion of the ceramic nanofillers in the epoxy composites. In a recent work by Ganguly et al. [43], the addition of ceramic in composites showed deterioration in the composite strength. This was due to the aggregation of the fillers and poor adhesion of the ceramic in the composites. This may be a similar reason to that for the current findings. The SEM observation shown in Figure 5 might assist in this analysis.

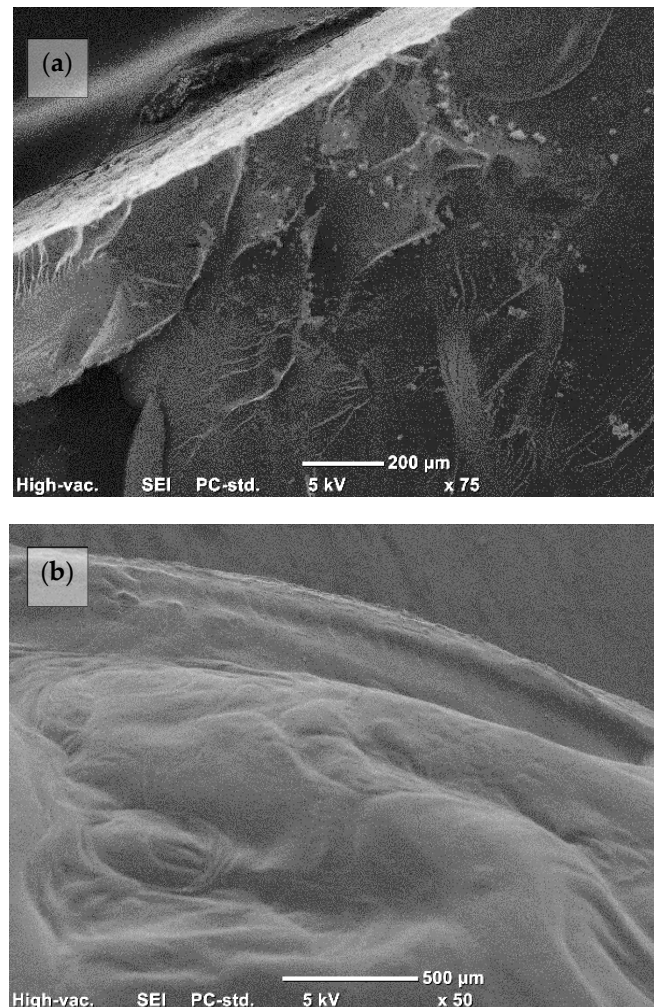


**Figure 5.** Micrographs of tensile samples of pure epoxy. (a) Micrographs showing brittle fracture of pure epoxy (b) micrographs showing river like pattern.

The incorporation of ceramic fillers into epoxy composites resulted in a noticeable decline in ultimate tensile strength. This phenomenon is consistent with previous studies on ceramic-reinforced composites, where the introduction of fillers, especially at higher concentrations, can lead to issues such as filler aggregation and weak interfacial bonding between the matrix and the filler materials [43,44]. These factors contribute to a reduction in mechanical properties like tensile strength. Despite the decrease in strength, it is important to note that the modulus of elasticity remained relatively stable across all ceramic content levels, indicating that the stiffness of the composites was not significantly affected. This trade-off between reduced strength and the enhanced wear resistance brought by ceramic fillers is a common feature in composite materials. It underscores the potential of

ceramic/epoxy composites for applications where improved tribological performance and structural rigidity are prioritized over tensile strength.

The addition of YSZ ceramic powder to the epoxy matrix decreases the composite's ultimate tensile strength, but it does not significantly alter the modulus of elasticity. This behavior can be explained by considering the different mechanisms that govern the strength and modulus in composite materials [45]. The tensile strength of a composite is highly dependent on the interaction between the matrix and the filler material. In this case, the relatively poor adhesion between the ceramic particles and the epoxy matrix, as well as the potential for particle agglomeration, leads to stress concentration points and microvoids, which reduce the overall strength of the composite [46–48]. These localized weaknesses allow cracks to initiate and propagate more easily, resulting in lower tensile strength. However, the modulus of elasticity is primarily a measure of the stiffness of the material and is less sensitive to defects at the microscopic level [49]. Since both the ceramic particles and the epoxy matrix are inherently stiff, the modulus remains relatively stable even as the ceramic content increases. This trade-off between reduced strength and stable stiffness has significant implications for the material's overall performance [50]. In applications where wear resistance and stiffness are critical, such as tribological systems, the reduction in tensile strength may be acceptable, provided that the material's modulus and wear resistance are maintained [51,52]. However, for structural applications requiring high strength, the observed reduction in tensile strength must be carefully considered when determining the suitability of the material.

Figures 5 and 6 show the failure to be of a brittle nature which is in line with the stress–strain trends curves presented in Figure 3. In Figure 5a,b, one can notice there is a clear fracture on the surface (Figure 5a). In Figure 5b, there is a river-like pattern which is evidence of the brittle nature of the epoxy. The presence of ceramic debris and voids on the surface of the 40% composite in Figure 5 indicates the lack of good adhesion of the ceramic with the epoxy resin. However, there is no remarkable evidence of aggregation of ceramic powder. This can be further studied to clearly understand the adhesion behavior of the ceramic powder in thermoset composites. Research conducted by Ray et al. [44] also reported a similar issue. However, in that work, different fillers were used in the vinyl ester which made it unclear whether the ceramic filler was the poor addition or the other fillers.

When it comes to the modulus, the addition of ceramic to an epoxy composite does not seem to have a significant impact. This is because the modulus values remain between 0.4 and 0.55 GPa for all composite variations. One possible explanation for this is that both ceramic and epoxy have a brittle nature, as noted in a previous study by Venturini et al. [53]. However, the ductility of the epoxy composite is affected by the addition of ceramic. In particular, the ductility of the pure epoxy is around 8%, while the ductility drops to 5.5% with the addition of 40% ceramic.

In Figure 6a,b, there are voids and detachment of ceramic particles. The observed voids and detachment of ceramic particles in the SEM micrograph of epoxy composites can be attributed to deformation in the epoxy matrix associated with the fact that the matrix cannot accommodate the stress adequately [54,55]. Stress concentration points arising from the presence of ceramic particles may initiate cracks, resulting in detachment. Inadequate adhesion between the matrix and ceramics, particle agglomeration, mechanical property mismatches, and aggressive loading conditions can further contribute to the observed failure mechanisms [56]. It is recommended to address this point through improved bonding and particle distribution for optimizing the composite's tensile strength and durability.

While both Ytria-Stabilized Zirconia (YSZ) and epoxy are brittle materials, incorporating YSZ into the epoxy matrix offers several significant advantages that outweigh the potential concern of brittleness. YSZ is known for its exceptional hardness, high wear resistance, and thermal stability, making it an ideal reinforcing filler for epoxy composites in applications where these properties are prioritized over toughness [57]. In tribological systems, for instance, the wear resistance provided by YSZ can significantly extend the lifespan of the material under sliding or abrasive conditions [58]. Additionally, the

incorporation of YSZ enhances the surface hardness of the composite, which can reduce material deformation and surface damage during frictional contact [59,60]. Although both materials are brittle, the overall performance of the composite is optimized for applications that require high stiffness, minimal deformation, and superior resistance to wear, rather than ductility. This makes the YSZ/epoxy composite particularly suitable for tribological applications where wear resistance is critical, even at the expense of some reduction in fracture toughness.

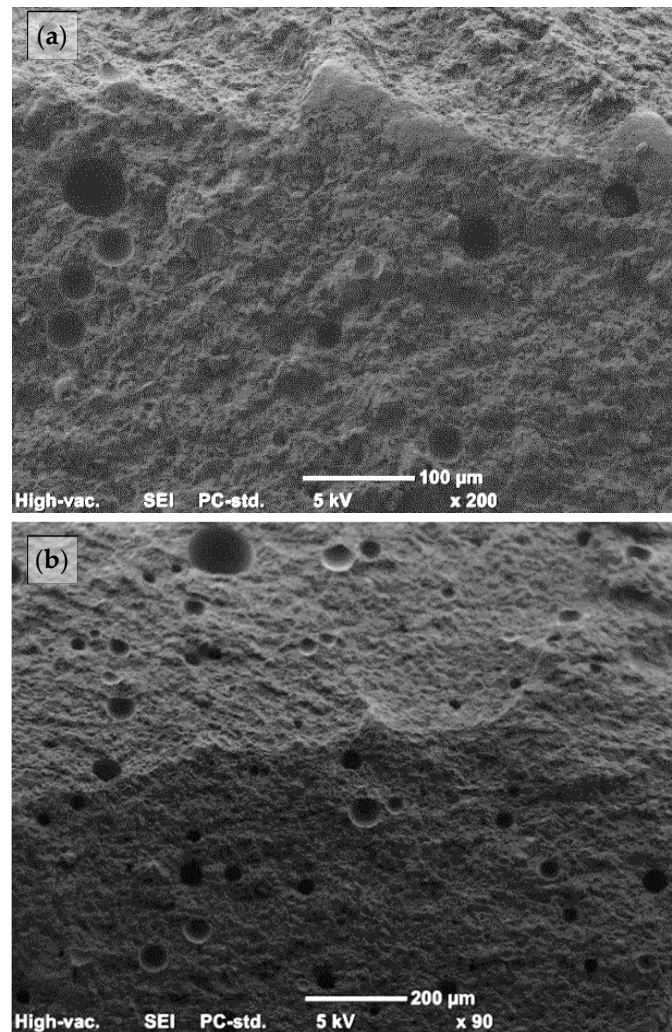


**Figure 6.** Micrographs of tensile samples of epoxy composite containing 40% ceramic. (a) High magnification of micrographs for the composites showing detachment and voids in the composites, (b) low magnification of the composites indicating void.

### 3.2. Tribological Results

Tribological experiments were conducted using a block-on-ring configuration. Epoxy composites with different contents of ceramics were evaluated against a stainless steel counterface. Figure 6 represents the specific wear rate of the composites at different sliding distances. The figures show that two stages of wear can be observed as running-in and steady-state stages. At about 5 km of the sliding distance, the steady state was initiated. However, from 2 km to 5 km of the sliding distance was the running-in stage. During the running-in stage, there is adhesion between the two surfaces (epoxy composites and stainless steel), i.e., the asperities of the epoxy composite surface interact with the stainless steel asperities. During this stage, there might be a film of epoxy composites generated

on the stainless steel surface; this might explain the high specific wear rate values of the composites at the running-in stage (between 2 and 5 km of the sliding distance).

The observed variations in the friction coefficient with increasing YSZ content in Figure 6 can be attributed to a combination of surface hardness, surface roughness, and particle–matrix interactions. As the YSZ content increases, the surface hardness of the composite also increases due to the inclusion of hard ceramic particles. At 20% YSZ content, this increase in hardness leads to reduced material deformation and wear, resulting in a lower friction coefficient [61,62]. However, as the ceramic content reaches 40%, the surface roughness of the composite increases due to the protrusion of ceramic particles from the matrix. This increased roughness causes more mechanical interlocking between the composite and the counterface, contributing to a higher friction coefficient. Additionally, the interaction between the epoxy matrix and YSZ particles changes as the ceramic content rises. At lower concentrations, the matrix plays a dominant role in the frictional behavior, keeping the coefficient relatively low [63,64]. As the ceramic content increases, the YSZ particles dominate the surface characteristics, introducing harder and more abrasive surfaces that contribute to the observed increase in the friction coefficient at 40%. These combined factors explain the trend in frictional behavior as YSZ content increases. On the other hand, the steady state indicates the stability of the rubbing area after exiting the running stage. In the design and material selection, the steady state is more important than the running in, since it represents the life performance of the components. Accordingly, the steady state of the composites is extracted and presented in Figure 7.

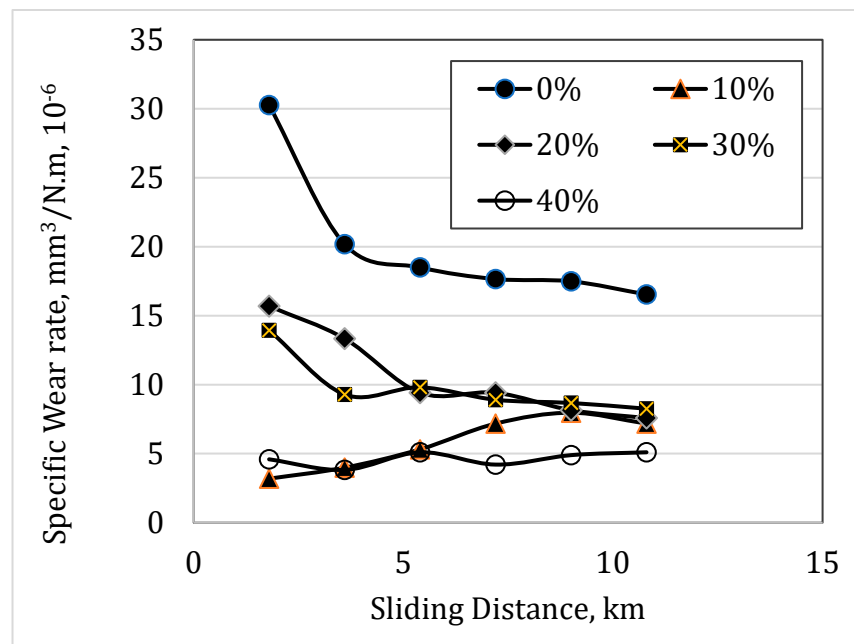


**Figure 7.** The specific wear rate of epoxy composites with different ceramic contents.

The specific wear rate values at the steady state of the epoxy composites with different contents are presented in Figure 8. It is clear that the addition of the ceramic dramatically decreases the specific wear rate, showing high resistance to wear. It should be mentioned here that the hardness of the ceramic is higher than that of the stainless steel, which may be the reason for the reduction in the specific wear rate. This is one of the fundamental thoughts of adhesive wear [20,65]. This will be further explained in the surface roughness test and SEM in the following sections.

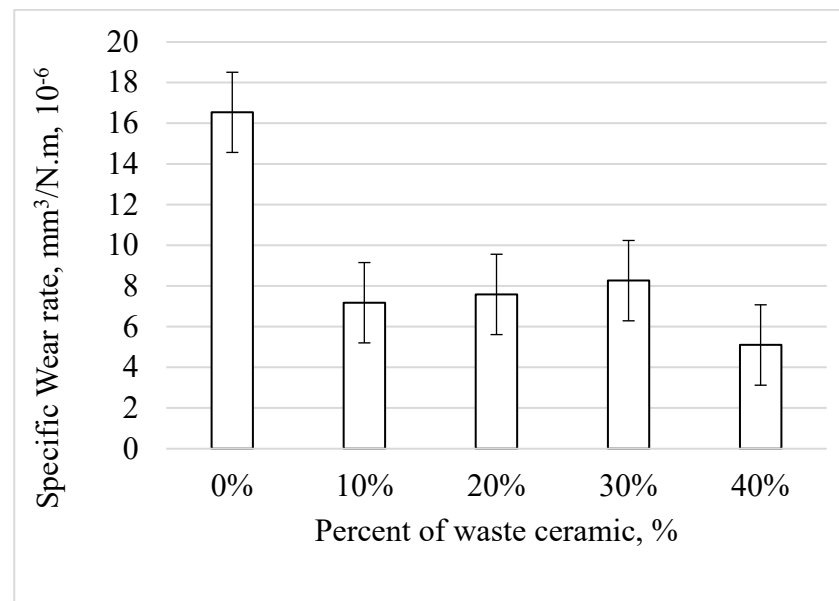


**Figure 8.** The specific wear rate of epoxy composites with different ceramic contents in the steady state.

The friction coefficient is an important property of composite materials, and the addition of ceramics to an epoxy matrix can affect this property. The friction coefficient of the epoxy composite containing different contents of ceramics is presented in Figure 9. The figure shows that pure epoxy has a high friction coefficient compared to its composites. Regarding the specific wear rate of pure epoxy (Figure 7), it is expected that the friction coefficient should be lower than its composites since the high amount of material removal from the surface represents less resistance to sliding (low friction coefficient). The current results oppose that thought. A similar phenomenon has been reported with pure thermoset materials such as epoxy [66,67] and polyester [68,69]. In those reported works, the sticking process took place in the rubbing area, which resulted in the high friction coefficient of pure thermosets. On the other hand, the high friction coefficient in the rubbing area associated with the shear force due to the sliding of the stainless steel counterface would result in high material removal from the softer surface (pure epoxy) [70]. This may explain the high friction coefficient and the specific wear rate of the pure epoxy.

Regarding the effect of the ceramic content on the frictional performance of the epoxy composites, Figure 9 shows that the high and low content of the ceramic results in a high friction coefficient. The high friction coefficient of the 10 wt.% ceramic in the epoxy is due to the same reason as the pure epoxy. In other words, the 10 wt.% of the ceramic in the composite does not influence the frictional behavior of the epoxy. With regard to the high content of ceramic in the epoxy (40 wt.%), some studies have shown that the friction coefficient of an epoxy composite can increase with the addition of hard fillers such as ceramic or diamond particles, due to the increased surface roughness and hardness of the composite surface [71,72].

Regarding the effect of the composite surface on the stainless steel counterface surface, Figure 10 displays the surface roughness of the counterface surface after the set of tests was completed. It should be mentioned here that the counterface surface was cleaned with acetone after the test completion and then the surface roughness measurement was performed. The figure shows the impact of the epoxy/ceramic surface on the counterface considering the different contents of ceramic. There is a clear proportional relation between the increase in the surface roughness with the increase in the ceramic content. This may be due to the high hardness of the ceramic compared to the stainless steel counterface [73].

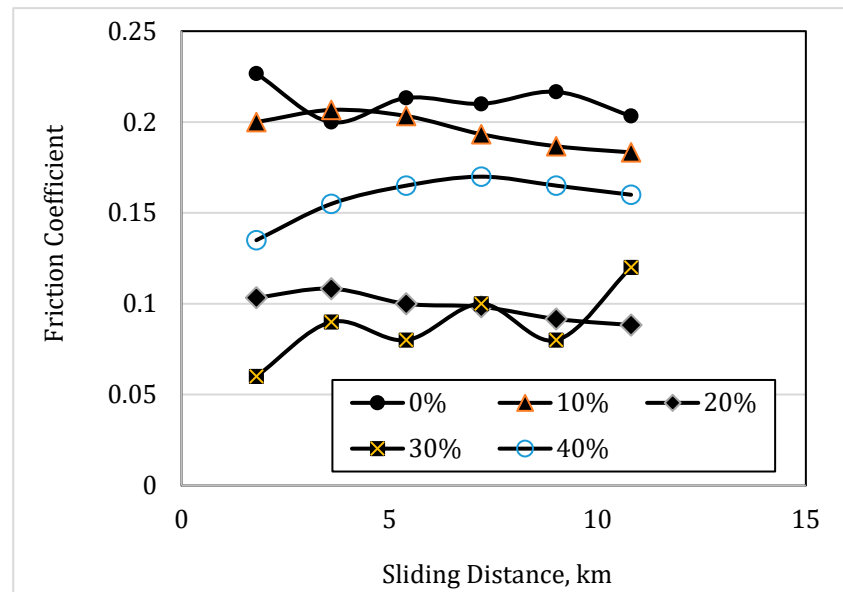


Figure 9. The friction coefficient of epoxy composites with different ceramic contents.

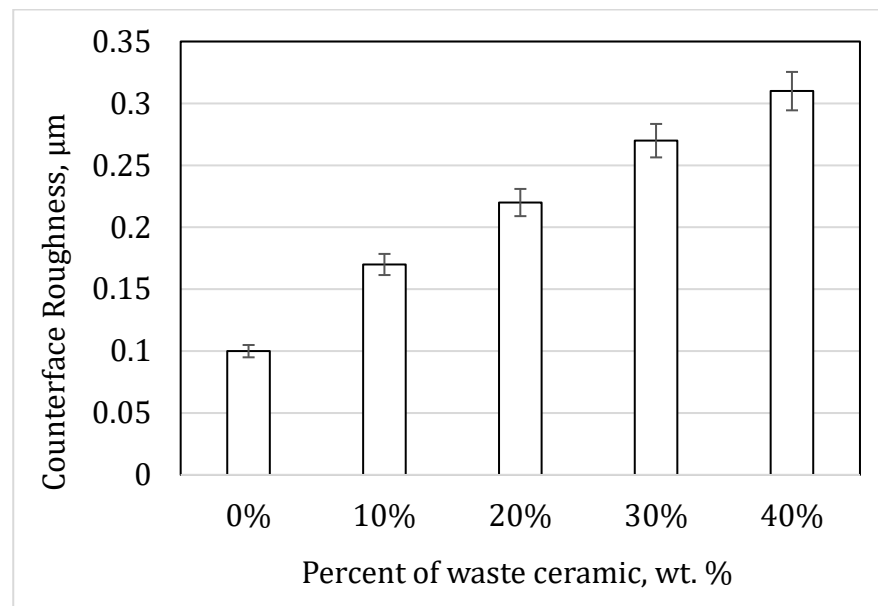
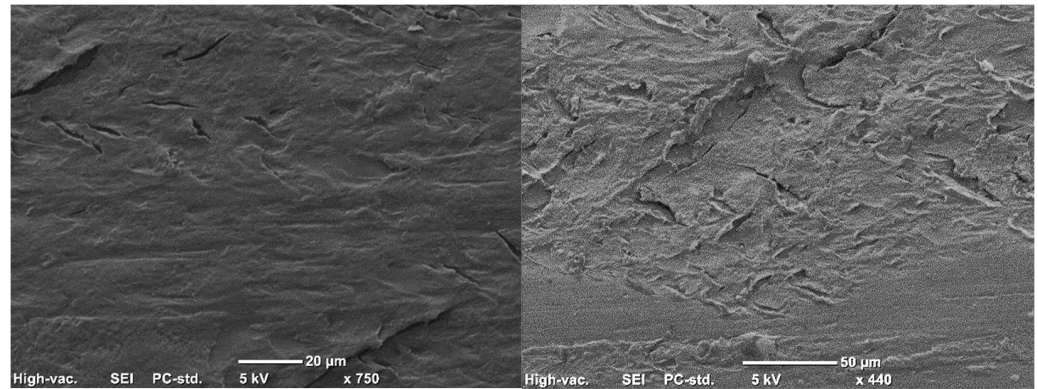


Figure 10. Counterface roughness after testing epoxy composites with different ceramic contents.

Further to the above thoughts, SEM observation was conducted on the worn surfaces of the composites after an 11 km sliding distance. Figure 11 shows the micrographs of the worn surface of pure epoxy. The micrographs show clear signs of plastic deformation and a river-like pattern toward the direction of the slide. In addition, there is a sign of micro/macrocracks. Such a wear mechanism has been reported previously when pure epoxy or polyester rubbed against metal surfaces [74,75]. Scanning electron microscopy (SEM) observations of epoxy/20% ceramic composites reveal the presence of abrasive patches on the surface, indicating the presence of ceramic particles in the composite, Figure 12. These patches are indicative of the abrasive nature of the ceramic particles and their effect on the surrounding epoxy matrix [76]. Additionally, SEM analysis also reveals the presence of film debris scattered across the surface, further highlighting the abrasive nature of the ceramic particles. SEM observations of epoxy/40% ceramic composites indicate the presence of large patches of film loss on the surface, which is due to the high

concentration of ceramic particles in the composite [77]. The SEM images also reveal the abrasive nature of the ceramic particles, which can cause damage to the surrounding epoxy matrix. These findings are consistent with previous studies on different fillers of hard material in thermoset composites, which have shown that increasing the filler content can lead to a higher degree of abrasion and wear [78,79].



**Figure 11.** Worn surface of pure epoxy.

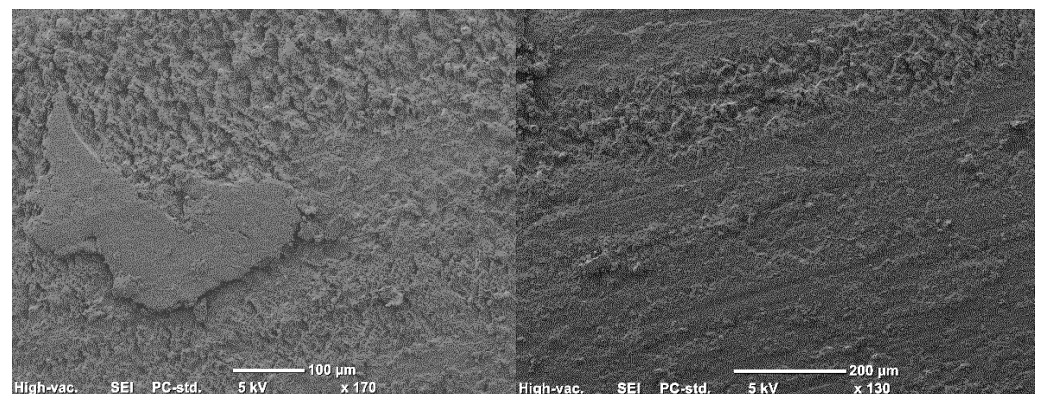


**Figure 12.** Worn surface of epoxy composites containing 20% ceramics.

Figure 13 delineates distinct layers observed on the surface, indicative of a transparent film affixed to the composite surface. During sliding interactions between the epoxy composites and metals, the interfacial zone experiences heat generation, causing softening of the epoxy region and subsequent detachment of ceramic particles [80]. This phenomenon results in the formation of a film on either the metal or composite surfaces. The weakened nature of this film makes it susceptible to detachment under shear loading conditions. Similar behavior has been documented in prior studies involving various epoxy composites, underscoring a recurring characteristic of the material response under analogous sliding conditions [81,82].

Up to the recent year, no similar work has been carried out addressing the influence of YSZ waste ceramic powder on the adhesive wear performance of epoxy composites. However, some works have been reported on either abrasive wear or macro-size ceramics. Accordingly, the current results will be compared with the up-to-date literature. In the most recent work by Upadhyay et al. [83], waste marble dust in epoxy composites was investigated. In terms of tensile properties, the increase in marble dust up to 40% increased the modulus to 5.5 GPa and reduced the tensile strength to 27 MPa. The current findings are almost similar despite there being fewer values. With regard to the tribological behavior, the marble dust/epoxy composites showed a specific wear rate in the range of 0.02–0.03 ( $10^{-5} \text{ mm}^3/\text{N.m}$ ), while the current results of the ceramic powder are 0.0005–0.00024 ( $10^{-5} \text{ mm}^3/\text{N.m}$ ). It should be mentioned here that the work in the literature was conducted

via abrasive loading while the current study is in adhesive mode. This shows that such materials can perform better under adhesive loading compared to abrasion.

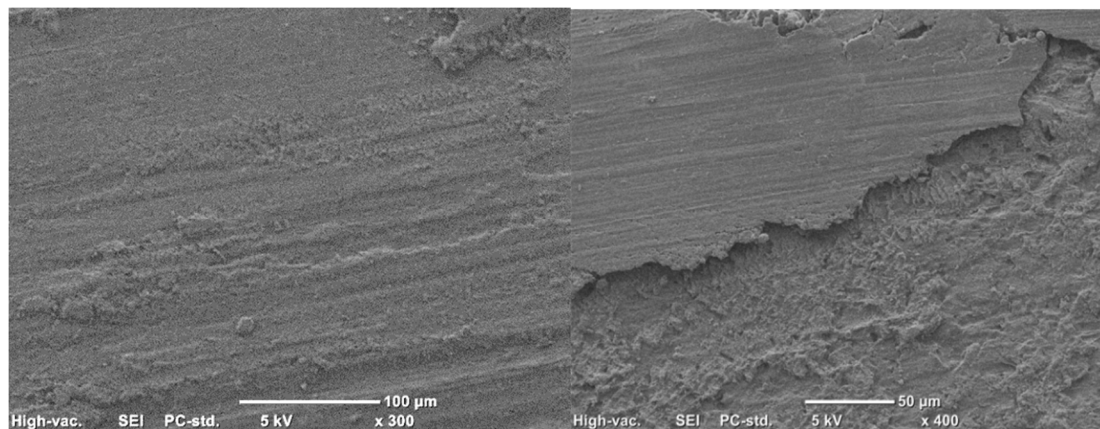


**Figure 13.** Worn surface of epoxy composites containing 40% ceramics.

### 3.3. Sustainability Aspects and Potential for Real-World Application

The use of ceramic waste in the production of epoxy composites offers significant environmental, social, and economic benefits [84]. From an environmental perspective, the reuse of ceramic waste reduces the need for landfill space and lowers the demand for virgin raw materials, thus conserving natural resources and minimizing the ecological footprint associated with material extraction and processing [85]. In addition, utilizing waste materials can lead to a reduction in energy consumption and emissions compared to traditional composite fabrication methods. Socially, promoting the use of waste materials aligns with the global shift toward sustainable engineering practices and corporate social responsibility, potentially generating new employment opportunities in the waste management and recycling sectors [86]. Economically, the incorporation of YSZ ceramic powder can lower production costs for industries by providing an affordable and sustainable alternative to conventional fillers [87]. This, in turn, can make eco-friendly composite materials more accessible to a wider range of industries, further promoting sustainability.

The findings of this study hold significant potential for real-world applications, particularly in industries where high wear resistance, surface hardness, and thermal stability are critical factors. The YSZ-reinforced epoxy composites could be highly beneficial in the automotive and aerospace industries, where components such as gears, bearings, and coatings are exposed to high friction and wear environments [88]. These materials can also find applications in industrial machinery, particularly in moving parts that require durable and wear-resistant surfaces. Additionally, the use of these composites in renewable energy systems, such as wind turbine components or protective coatings for solar panels, can extend the operational lifespan of these technologies while promoting the use of sustainable materials. By incorporating waste-derived YSZ ceramics, these composites provide an eco-friendly solution to material challenges in high-performance industries, contributing to both improved product performance and reduced environmental impact.

## 4. Conclusions

In conclusion, this study demonstrated the potential of waste-derived Yttria-Stabilized Zirconia (YSZ) as a reinforcing filler in epoxy composites. The addition of YSZ significantly influenced the mechanical and tribological properties of the composites. Specifically, the tensile strength of the composites decreased by approximately 15% when the ceramic content was increased from 0 wt.% to 40 wt.%. However, the wear resistance of the composites improved substantially, with a 30% reduction in the wear rate observed at 20 wt.% YSZ content. Furthermore, the friction coefficient increased by approximately 25% at the highest YSZ content (40 wt.%), reflecting the increased hardness and abrasive nature of the

ceramic filler. The optimal ceramic content for achieving a balance between mechanical strength and wear resistance was found to be 20 wt.%, where the composite maintained sufficient tensile strength while exhibiting significantly enhanced wear resistance. These findings indicate that YSZ-reinforced epoxy composites are suitable for industrial applications where wear resistance and surface hardness are critical. Future research should focus on improving the interfacial adhesion between the YSZ particles and the epoxy matrix, potentially through surface treatments or coupling agents, to further enhance the material's mechanical performance.

**Author Contributions:** Formal analysis, A.E.A.; Investigation, T.A.; Writing—original draft, B.F.Y.; Writing—review and editing, J.G.A. and V.G. All authors have read and agreed to the published version of the manuscript.

**Funding:** This research received no external funding.

**Data Availability Statement:** The original contributions presented in the study are included in the article, further inquiries can be directed to the corresponding author.

**Conflicts of Interest:** The authors declare no conflict of interest.

## References

1. Aoki-Suzuki, C.; Dente, S.M.R.; Hashimoto, S. Assessing economy-wide eco-efficiency of materials produced in Japan. *Resour. Conserv. Recycl.* **2023**, *194*, 106981. [\[CrossRef\]](#)
2. Shalwan, A.; Alajmi, A.; Yousif, B. Theoretical Study of the Effect of Fibre Porosity on the Heat Conductivity of Reinforced Gypsum Composite Material. *Polymers* **2022**, *14*, 3973. [\[CrossRef\]](#) [\[PubMed\]](#)
3. Bello, S.; Agunsoye, J.; Hassan, S.; Kana, M.Z. Epoxy resin based composites, mechanical and tribological properties: A review. *Tribol. Ind.* **2015**, *37*, 500.
4. Mahamude, A.S.F.; Harun, W.S.W.; Kadirgama, K.; Farhana, K.; Ramasamy, D.; Samylingam, L.; Aslfattahi, N. Thermal performance of nanomaterial in solar collector: State-of-play for graphene. *J. Energy Storage* **2021**, *42*, 103022. [\[CrossRef\]](#)
5. Hegab, H.; Khanna, N.; Monib, N.; Salem, A. Design for sustainable additive manufacturing: A review. *Sustain. Mater. Technol.* **2023**, *35*, e00576. [\[CrossRef\]](#)
6. Javaid, M.; Haleem, A.; Singh, R.P.; Khan, S.; Suman, R. Sustainability 4.0 and its applications in the field of manufacturing. *Internet Things Cyber-Phys. Syst.* **2022**, *2*, 82–90. [\[CrossRef\]](#)
7. Ramadan, M.; Reda, R. Cnts, Al<sub>2</sub>O<sub>3</sub> and SiO<sub>2</sub> reinforced epoxy: Tribological properties of polymer nanocomposites. *Tribol. Ind.* **2017**, *39*, 357. [\[CrossRef\]](#)
8. Samylingam, I.; Kadirgama, K.; Aslfattahi, N.; Samylingam, L.; Ramasamy, D.; Harun, W.; Samykano, M.; Saidur, R. Review on thermal energy storage and eutectic nitrate salt melting point. *IOP Conf. Ser. Mater. Sci. Eng.* **2021**, *1078*, 012034. [\[CrossRef\]](#)
9. Zou, W.; Zhang, W.; Pi, Y.; Zhang, Y.; Chen, Y.; Zhang, L. Study on preparation of glass-ceramics from multiple solid waste and coupling mechanism of heavy metals. *Ceram. Int.* **2022**, *48*, 36166–36177. [\[CrossRef\]](#)
10. Er, Y.; Sutcu, M.; Gencel, O.; Totiç, E.; Erdogmus, E.; Cay, V.V.; Munir, M.J.; Kazmi, S.M.S. Recycling of metallurgical wastes in ceramics: A sustainable approach. *Constr. Build. Mater.* **2022**, *349*, 128713. [\[CrossRef\]](#)
11. Xia, F.; Cui, S.; Pu, X. Performance study of foam ceramics prepared by direct foaming method using red mud and K-feldspar washed waste. *Ceram. Int.* **2022**, *48*, 5197–5203. [\[CrossRef\]](#)
12. Awoyera, P.O.; Olalusi, O.B.; Babagbale, D.P. Production of lightweight mortar using recycled waste papers and pulverized ceramics: Mechanical and microscale properties. *J. Build. Eng.* **2021**, *39*, 102233. [\[CrossRef\]](#)
13. Pommer, V.; Vejmelková, E.; Černý, R.; Keppert, M. Alkali-activated waste ceramics: Importance of precursor particle size distribution. *Ceram. Int.* **2021**, *47*, 31574–31582. [\[CrossRef\]](#)
14. Zhang, G.-Y.; Lin, R.-S.; Wang, X.-Y. Effect of waste oyster shell powder on the properties of alkali-activated slag–waste ceramic geopolymers. *J. Mater. Res. Technol.* **2023**, *22*, 1768–1780. [\[CrossRef\]](#)
15. Huang, Z.-H.; Li, J.; Li, L.-X.; Xu, H.-M.; Han, C.; Liu, M.-Q.; Xiang, J.; Shen, X.-Q.; Jing, M.-X. Boosting lithium-ion transport capability of LAGP/PPO composite solid electrolyte via component regulation from ‘Ceramics-in-Polymer’ to ‘Polymer-in-Ceramics’. *Ceram. Int.* **2022**, *48*, 25949–25957. [\[CrossRef\]](#)
16. Shinyjoy, E.; Ramya, S.; Saravanakumar, P.; Manoravi, P.; Kavitha, L.; Gopi, D. Chapter 28—Naturally derived ceramics–polymer composite for biomedical applications. In *Advances in Biomedical Polymers and Composites*; Pal, K., Verma, S., Datta, P., Barui, A., Hashmi, S.A.R., Srivastava, A.K., Eds.; Elsevier: Amsterdam, The Netherlands, 2023; pp. 711–743.
17. Zhao, S.; Chen, J.; Yang, F.; Chen, G.; Zhang, L.; Yang, Z. Microstructural evolution of polymer derived SiC ceramics and SiC/SiC composite under 1.8MeV electron irradiation. *J. Nucl. Mater.* **2023**, *580*, 154408. [\[CrossRef\]](#)
18. Robinson, J.L.; Brudnicki, P.; Lu, H.H. 1.21 Polymer-Bioactive Ceramic Composites. In *Comprehensive Biomaterials II*; Ducheyne, P., Ed.; Elsevier: Oxford, UK, 2017; pp. 460–477.
19. Yousif, B.F. Editorial for SI: Materials, design and tribology. *Mater. Des.* **2013**, *48*, 1. [\[CrossRef\]](#)

20. Yousif, B.F. Design of newly fabricated tribological machine for wear and frictional experiments under dry/wet condition. *Mater. Des.* **2013**, *48*, 2–13. [[CrossRef](#)]
21. Katiyar, J.K.; Ruggiero, A.; Rao, T.; Davim, J.P. *Industrial Tribology: Sustainable Machinery and Industry 4.0*; CRC Press: Boca Raton, FL, USA, 2022.
22. Kumar, R.; Samykano, M.; Pandey, A.; Kadirgama, K.; Tyagi, V. A comparative study on thermophysical properties of functionalized and non-functionalized Multi-Walled Carbon Nano Tubes (MWCNTs) enhanced salt hydrate phase change material. *Sol. Energy Mater. Sol. Cells* **2022**, *240*, 111697.
23. Samyalingam, L.; Aslfattahi, N.; Kok, C.K.; Kadirgama, K.; Sazali, N.; Liew, K.W.; Schmirler, M.; Ramasamy, D.; Harun, W.S.W.; Samykano, M. Enhancing Lubrication Efficiency and Wear Resistance in Mechanical Systems through the Application of Nanofluids: A Comprehensive Review. *J. Adv. Res. Micro Nano Eng.* **2024**, *16*, 1–18. [[CrossRef](#)]
24. Panchal, M.; Minugu, O.P.; Gujjala, R.; Ojha, S.; Mallampati Chowdary, S.; Mohammad, A. Study of environmental behavior and its effect on solid particle erosion behavior of hierarchical porous activated carbon-epoxy composite. *Polym. Compos.* **2022**, *43*, 2276–2287. [[CrossRef](#)]
25. Shiv, J.K.; Kumar, K.; Jayapalan, S. Recent advances in polymer using metal oxides nanocomposite and its hybrid fillers for tribological application. *Adv. Mater. Process. Technol.* **2023**, 1–12. [[CrossRef](#)]
26. Amurin, L.G.; Felisberto, M.D.; Ferreira, F.L.; Soraes, P.H.; Oliveira, P.N.; Santos, B.F.; Valeriano, J.C.; de Miranda, D.C.; Silva, G.G. Multifunctionality in ultra high molecular weight polyethylene nanocomposites with reduced graphene oxide: Hardness, impact and tribological properties. *Polymer* **2022**, *240*, 124475. [[CrossRef](#)]
27. Luo, P.; Zhang, J.; You, Z.; Ran, X.; Liu, Y.; Li, S.; Li, S. Effect of TiO<sub>2</sub> content on the microstructure and mechanical and wear properties of yttria-stabilized zirconia ceramics prepared by pressureless sintering. *Mater. Res. Express* **2020**, *6*, 125211. [[CrossRef](#)]
28. He, Y.; Zhang, S.; He, Y.; Song, R.; Zhang, Z.; Liu, B.; Li, H.; Shangguan, J. Effects of yttrium-stabilized zirconia (different yttrium content) doping on the structure, corrosion resistance and wear resistance of Ni-P electroless coating. *Colloids Surf. A Physicochem. Eng. Asp.* **2022**, *654*, 130059. [[CrossRef](#)]
29. Jadhav, P.M.; Kumar Reddy, N.S. Wear behavior of carbide tool coated with Yttria-stabilized zirconia nano particles. *IOP Conf. Ser. Mater. Sci. Eng.* **2018**, *346*, 012007. [[CrossRef](#)]
30. Ramachandran, K.; Ramasamy, D.; Samykano, M.; Samyalingam, L.; Tarlochan, F.; Najafi, G. Evaluation of specific heat capacity and density for cellulose nanocrystal-based nanofluid. *J. Adv. Res. Fluid Mech. Therm. Sci.* **2018**, *51*, 169–186.
31. Samykano, M.; Kananathan, J.; Kadirgama, K.; Amirruddin, A.; Ramasamy, D.; Samyalingam, L. Characterisation, Performance and Optimisation of Nanocellulose Metalworking Fluid (MWF) for Green Machining Process. *Int. J. Automot. Mech. Eng.* **2021**, *18*, 9188–9207. [[CrossRef](#)]
32. ASTM D638; Standard Test Method for Tensile Properties of Plastics. ASTM International: West Conshohocken, PA, USA, 2022.
33. ASTM G99; Standard Test Method for Wear Testing with a Pin-on-Disk Apparatus. ASTM International: West Conshohocken, PA, USA, 2023.
34. Ahmed, F.; Khanam, A.; Samyalingam, L.; Aslfattahi, N.; Saidur, R. Assessment of thermo-hydraulic performance of MXene-based nanofluid as coolant in a dimpled channel: A numerical approach. *J. Therm. Anal. Calorim.* **2022**, *147*, 12669–12692. [[CrossRef](#)]
35. Rangaswamy, H.; Chandrashekarappa, M.P.G.; Pimenov, D.Y.; Giasin, K.; Wojciechowski, S. Experimental investigation and optimization of compression moulding parameters for MWCNT/glass/kevlar/epoxy composites on mechanical and tribological properties. *J. Mater. Res. Technol.* **2021**, *15*, 327–341. [[CrossRef](#)]
36. Tavadi, A.R.; Nagabhushana, N.; Vivek Bhandarkar, V.; Jagadeesha, T.; Kerur, M.R.; Rudresha, S.; Durga Prasad, C.; Rajesh Kannan, A.; Mohan, D.G. Investigation on mechanical and sliding wear behavior of pongamia-oil-cake/basalt fiber-reinforced epoxy hybrid composites. *Arab. J. Sci. Eng.* **2024**, *49*, 2311–2325. [[CrossRef](#)]
37. Punj, S.; Singh, J.; Singh, K. Ceramic biomaterials: Properties, state of the art and future perspectives. *Ceram. Int.* **2021**, *47*, 28059–28074. [[CrossRef](#)]
38. El-Dieb, A.S.; Kanaan, D.M. Ceramic waste powder an alternative cement replacement—Characterization and evaluation. *Sustain. Mater. Technol.* **2018**, *17*, e00063. [[CrossRef](#)]
39. Andreola, F.; Barbieri, L.; Lancellotti, I.; Leonelli, C.; Manfredini, T. Recycling of industrial wastes in ceramic manufacturing: State of art and glass case studies. *Ceram. Int.* **2016**, *42*, 13333–13338. [[CrossRef](#)]
40. Ritchie, R.O. Toughening materials: Enhancing resistance to fracture. *Philos. Trans. R. Soc. A* **2021**, *379*, 20200437. [[CrossRef](#)]
41. Zhang, J.-Z.; Zhou, X.-P. Fracture process zone (FPZ) in quasi-brittle materials: Review and new insights from flawed granite subjected to uniaxial stress. *Eng. Fract. Mech.* **2022**, *274*, 108795. [[CrossRef](#)]
42. Ghazal, A.A. The Process of Maintenance and Assessment of The Universal Testing Material Machine H50KS. *J Mater Sci Appl* **2020**, *4*, 1–12.
43. Ganguly, D.; Bera, A.; Hore, R.; Khanra, S.; Maji, P.K.; Kotnees, D.K.; Chattopadhyay, S. Coining the attributes of nano to micro dual hybrid silica-ceramic waste filler based green HNBR composites for triple percolation: Mechanical properties, thermal, and electrical conductivity. *Chem. Eng. J. Adv.* **2022**, *11*, 100338. [[CrossRef](#)]
44. Ray, D.; Bhattacharya, D.; Mohanty, A.K.; Drzal, L.T.; Misra, M. Static and dynamic mechanical properties of vinyl ester resin matrix composites filled with fly ash. *Macromol. Mater. Eng.* **2006**, *291*, 784–792. [[CrossRef](#)]
45. Talreja, R.; Waas, A.M. Concepts and definitions related to mechanical behavior of fiber reinforced composite materials. *Compos. Sci. Technol.* **2022**, *217*, 109081. [[CrossRef](#)]

46. Anamalai, K.; Samyalingam, L.; Kadirgama, K.; Samykano, M.; Najafi, G.; Ramasamy, D.; Rahman, M. Multi-objective optimization on the machining parameters for bio-inspired nanocoolant. *J. Therm. Anal. Calorim.* **2019**, *135*, 1533–1544. [[CrossRef](#)]
47. Samsudin, S.S.; Abdul Majid, M.S.; Mohd Jamir, M.R.; Osman, A.F.; Jaafar, M.; Alshahrani, H.A. Physical, thermal transport, and compressive properties of epoxy composite filled with graphitic-and ceramic-based thermally conductive nanofillers. *Polymers* **2022**, *14*, 1014. [[CrossRef](#)]
48. Abd-Elaziem, W.; Khedr, M.; Elsheikh, A.H.; Liu, J.; Zeng, Y.; Sebae, T.A.; Abd El-Baky, M.A.; Darwish, M.A.; Daoush, W.M.; Li, X. Influence of nanoparticles addition on the fatigue failure behavior of metal matrix composites: Comprehensive review. *Eng. Fail. Anal.* **2023**, *155*, 107751. [[CrossRef](#)]
49. Liu, M.; Li, X. Mechanical properties measurement of materials and devices at micro-and nano-scale by optical methods: A review. *Opt. Lasers Eng.* **2022**, *150*, 106853. [[CrossRef](#)]
50. Mukherjee, G. Matrices for Composite Materials: Polymers, Metals, Ceramics, and Cements. In *Toughened Composites*; CRC Press: Boca Raton, FL, USA, 2022; pp. 81–99.
51. Pesode, P.; Barve, S. Comparison and performance of  $\alpha$ ,  $\alpha + \beta$  and  $\beta$  titanium alloys for biomedical applications. *Surf. Rev. Lett.* **2023**, *30*, 2330012. [[CrossRef](#)]
52. Eaki, M.; Kadirgama, K.; Abou El Hossein, K.; Samyalingam, L.; Kok, C. Enhancing Machining performance in Stainless Steel Machining using MXene Coolant: A Detailed Examination. *Int. J. Automot. Mech. Eng.* **2024**, *21*, 10993–11009. [[CrossRef](#)]
53. Venturini, A.B.; Prochnow, C.; Pereira, G.K.; Segala, R.D.; Kleverlaan, C.J.; Valandro, L.F. Fatigue performance of adhesively cemented glass-, hybrid-and resin-ceramic materials for CAD/CAM monolithic restorations. *Dent. Mater.* **2019**, *35*, 534–542. [[CrossRef](#)]
54. Kadirgama, K.; Samyalingam, L.; Aslfattahi, N.; Samykano, M.; Ramasamy, D.; Saidur, R. Experimental investigation on the optical and stability of aqueous ethylene glycol/mxene as a promising nanofluid for solar energy harvesting. *IOP Conf. Ser. Mater. Sci. Eng.* **2021**, *1062*, 012022. [[CrossRef](#)]
55. Gonçalves, P.T.; Arteiro, A.; Rocha, N.; Pina, L. Numerical analysis of micro-residual stresses in a carbon/epoxy polymer matrix composite during curing process. *Polymers* **2022**, *14*, 2653. [[CrossRef](#)]
56. Fernandes de Castro, E.; Bomfim Azevedo, V.L.; Nima, G.; Scopin de Andrade, O.; dos Santos Dias, C.T.; Giannini, M. Adhesion, Mechanical Properties, and Microstructure of Resin-matrix CAD-CAM Ceramics. *J. Adhes. Dent.* **2020**, *22*, 421–431.
57. Bapat, R.A.; Yang, H.J.; Chaubal, T.V.; Dharmadhikari, S.; Abdulla, A.M.; Arora, S.; Rawal, S.; Kesharwani, P. Review on synthesis, properties and multifarious therapeutic applications of nanostructured zirconia in dentistry. *RSC Adv.* **2022**, *12*, 12773–12793. [[CrossRef](#)]
58. Chandra, K.S.; Sarkar, D. Ceramic Coatings. In *Ceramic Processing*; CRC Press: Boca Raton, FL, USA, 2019; pp. 133–166.
59. Hisham, S.; Kadirgama, K.; Alotaibi, J.G.; Alajmi, A.E.; Ramasamy, D.; Sazali, N.; Kamarulzaman, M.K.; Yusaf, T.; Samyalingam, L.; Aslfattahi, N. Enhancing stability and tribological applications using hybrid nanocellulose-copper (II) oxide (CNC-CuO) nanolubricant: An approach towards environmental sustainability. *Tribol. Int.* **2024**, *194*, 109506. [[CrossRef](#)]
60. Samyalingam, L.; Anamalai, K.; Kadirgama, K.; Samykano, M.; Ramasamy, D.; Noor, M.; Najafi, G.; Rahman, M.; Xian, H.W.; Sidik, N.A.C. Thermal analysis of cellulose nanocrystal-ethylene glycol nanofluid coolant. *Int. J. Heat Mass Transf.* **2018**, *127*, 173–181. [[CrossRef](#)]
61. Kadirgama, K.; Noor, M.; Rahman, M.; Rejab, M.; Haron, C.; Abou-El-Hossein, K.A. Surface roughness prediction model of 6061-T6 aluminium alloy machining using statistical method. *Eng. Technol. Horiz.* **2020**, *33*, 77–83.
62. Zhai, W.; Bai, L.; Zhou, R.; Fan, X.; Kang, G.; Liu, Y.; Zhou, K. Recent progress on wear-resistant materials: Designs, properties, and applications. *Adv. Sci.* **2021**, *8*, 2003739. [[CrossRef](#)]
63. Kadirgama, K.; Noor, M.; Rahman, M. Optimization of surface roughness in end milling using potential support vector machine. *Arab. J. Sci. Eng.* **2012**, *37*, 2269–2275. [[CrossRef](#)]
64. Singh, J. Fabrication characteristics and tribological behavior of Al/SiC/Gr hybrid aluminum matrix composites: A review. *Friction* **2016**, *4*, 191–207. [[CrossRef](#)]
65. Cui, S.; Liu, Y.; Wang, T.; Tieu, K.; Wang, L.; Zeng, D.; Li, Z.; Li, W. Tribological behavior comparisons of high chromium stainless and mild steels against high-speed steel and ceramics at high temperatures. *Friction* **2022**, *10*, 436–453. [[CrossRef](#)]
66. Shalwan, A.; Yousif, B.F. Influence of date palm fibre and graphite filler on mechanical and wear characteristics of epoxy composites. *Mater. Des.* **2014**, *59*, 264–273. [[CrossRef](#)]
67. Yousif, B.F. 12—Tribological properties of biomass-based composites. In *Lignocellulosic Fibre and Biomass-Based Composite Materials*; Jawaid, M., Md Tahir, P., Saba, N., Eds.; Woodhead Publishing: Sawston, UK, 2017; pp. 225–257.
68. Albdiry, M.T.; Yousif, B.F. Morphological structures and tribological performance of unsaturated polyester based untreated/silane-treated halloysite nanotubes. *Mater. Des.* **2013**, *48*, 68–76. [[CrossRef](#)]
69. Alsaeed, T.; Yousif, B.F.; Ku, H. The potential of using date palm fibres as reinforcement for polymeric composites. *Mater. Des.* **2013**, *43*, 177–184. [[CrossRef](#)]
70. Rahman, M.; Ibrahim, T.K.; Kadirgama, K.; Mamat, R.; Bakar, R.A. Influence of operation conditions and ambient temperature on performance of gas turbine power plant. *Adv. Mater. Res.* **2011**, *189*, 3007–3013. [[CrossRef](#)]
71. Fouly, A.; Alkalla, M.G. Effect of low nanosized alumina loading fraction on the physico-mechanical and tribological behavior of epoxy. *Tribol. Int.* **2020**, *152*, 106550. [[CrossRef](#)]

72. Aghamohammadi, H.; Heidarpour, A.; Jamshidi, R.; Bayat, O. Tribological behavior of epoxy composites filled with nanodiamond and  $Ti_3AlC_2TiC$  particles: A comparative study. *Ceram. Int.* **2019**, *45*, 9106–9113. [[CrossRef](#)]
73. Yin, F.-I.; Ji, H.; Nie, S.-I. Tribological behavior of various ceramic materials sliding against CF/PTFE/graphite-filled PEEK under seawater lubrication. *Proc. Inst. Mech. Eng. Part J J. Eng. Tribol.* **2019**, *233*, 1729–1742. [[CrossRef](#)]
74. Nirmal, U.; Yousif, B.; Rilling, D.; Brevorn, P. Effect of betelnut fibres treatment and contact conditions on adhesive wear and frictional performance of polyester composites. *Wear* **2010**, *268*, 1354–1370. [[CrossRef](#)]
75. Narish, S.; Yousif, B.; Rilling, D. Adhesive wear of thermoplastic composite based on kenaf fibres. *Proc. Inst. Mech. Eng. Part J J. Eng. Tribol.* **2011**, *225*, 101–109. [[CrossRef](#)]
76. Muthusamy, Y.; Kadirgama, K.; Rahman, M.; Ramasamy, D.; Sharma, K. Wear analysis when machining AISI 304 with ethylene glycol/ $TiO_2$  nanoparticle-based coolant. *Int. J. Adv. Manuf. Technol.* **2016**, *82*, 327–340. [[CrossRef](#)]
77. Kadirgama, K.; Anamalai, K.; Ramachandran, K.; Ramasamy, D.; Samykano, M.; Kottasamy, A.; Lingenthiran; Rahman, M. Thermal analysis of SUS 304 stainless steel using ethylene glycol/nanocellulose-based nanofluid coolant. *Int. J. Adv. Manuf. Technol.* **2018**, *97*, 2061–2076. [[CrossRef](#)]
78. Engels, T. 8—Thermoset adhesives: Epoxy resins, acrylates and polyurethanes. In *Thermosets*; Guo, Q., Ed.; Woodhead Publishing: Sawston, UK, 2012; pp. 228–253.
79. Pujar, V.; Devarajaiah, R.M.; Suresha, B.; Bharat, V. A review on mechanical and wear properties of fiber-reinforced thermoset composites with ceramic and lubricating fillers. *Mater. Today Proc.* **2021**, *46*, 7701–7710. [[CrossRef](#)]
80. Samyalingam, I.; Kadirgama, K.; Samyalingam, L.; Aslfattahi, N.; Ramasamy, D.; Sazali, N.; Harun, W.S.W.; Kok, C.K. Review of  $Ti_3C_2Tx$  MXene Nanofluids: Synthesis, Characterization, and Applications. *Eng. Technol. Appl. Sci. Res.* **2024**, *14*, 14708–14712. [[CrossRef](#)]
81. Alotaibi, J.G.; Eid Alajmi, A.; Mehoub, G.A.; Yousif, B.F. Epoxy and polyester composites' characteristics under tribological loading conditions. *Polymers* **2021**, *13*, 2230. [[CrossRef](#)]
82. Eayal Awwad, K.; Yousif, B.; Fallahnezhad, K.; Saleh, K.; Zeng, X. Influence of graphene nanoplatelets on mechanical properties and adhesive wear performance of epoxy-based composites. *Friction* **2021**, *9*, 856–875. [[CrossRef](#)]
83. Upadhyay, P.; Rajput, V.; Singh Rajput, P.; Mishra, V.; Ahmad Khan, I.; Jha, A.; Agrawal, A. Physical, mechanical and sliding wear behaviour of epoxy composites filled with micro-sized marble dust composites. *Mater. Today Proc.* **2023**, *in press*. [[CrossRef](#)]
84. Sandanamsamy, L.; Harun, W.; Ishak, I.; Romlay, F.; Kadirgama, K.; Ramasamy, D.; Idris, S.; Tsumori, F. A comprehensive review on fused deposition modelling of polylactic acid. *Prog. Addit. Manuf.* **2023**, *8*, 775–799. [[CrossRef](#)]
85. Samyalingam, L.; Aslfattahi, N.; Kok, C.K.; Kadirgama, K.; Sazali, N.; Schmirler, M.; Ramasamy, D.; Harun, W.S.W.; Samykano, M.; Veerendra, A. Green Engineering with Nanofluids: Elevating Energy Efficiency and Sustainability. *J. Adv. Res. Micro Nano Eng.* **2024**, *16*, 19–34. [[CrossRef](#)]
86. Sondh, S.; Upadhyay, D.S.; Patel, S.; Patel, R.N. Strategic approach towards sustainability by promoting circular economy-based municipal solid waste management system-A review. *Sustain. Chem. Pharm.* **2024**, *37*, 101337. [[CrossRef](#)]
87. Kumar, R.; Pandey, R.K.; Shukla, S.S.; Gidwani, B. Ceramic Fillers, Fibers, and Acrylics. In *Magnetic Polymer Composites and Their Emerging Applications*; CRC Press: Boca Raton, FL, USA, 2024; pp. 289–313.
88. Ghandvar, H.; Farahany, S.; Bakar, T.A.A. A novel method to enhance the performance of an ex-situ Al/Si-YSZ metal matrix composite. *J. Alloys Compd.* **2020**, *823*, 153673. [[CrossRef](#)]

**Disclaimer/Publisher's Note:** The statements, opinions and data contained in all publications are solely those of the individual author(s) and contributor(s) and not of MDPI and/or the editor(s). MDPI and/or the editor(s) disclaim responsibility for any injury to people or property resulting from any ideas, methods, instructions or products referred to in the content.